

Synthesized activated carbon derived from discarded styrofoam and effectively removal of nickel (II) from aqueous solutions

Roopa Dakshinamurthy¹ , Balasundaram Natarajan¹, Meiaraj Chelladurai²

¹Karpagam Academy of Higher Education, Faculty of Engineering, Department of Civil Engineering, Coimbatore, Tamil Nadu, India.

²Government College of Technology, Coimbatore, Tamil Nadu, India.

e-mail: roopa2karthik@gmail.com, balasundaram49@gmail.com, cmeiaraj@gmail.com

ABSTRACT

Due to the rapid urbanisation and rapid population explosion, there is a vast essential requirement in the dispose of solid waste. Carbonization of Styrofoam is carried out at varying temperature ranges of 300°C to 675°C at an interval of 75°C using KOH as reagent. The Characterisation of power of hydrogen ion, ash and moisture content, fixed carbon, Volatile matter, iodine adsorption value, methyl blue value was conducted. It was found that the activate carbon obtain from the temperature of 525°C has a good carbon characteristic. The batch experiment such as pH, contact time, carbon dosage, agitation speed, potency of Nickel (II) was conducted with the purpose of ascertaining the efficiency of Nickel (II) adsorption. This analysis deals with fixed bed column to remove Nickel (II) from a solution. The results indicated that the sorption-second order kinetic model was the most appropriate fit for the data, and alternative models such as Adams-Bhorat, Thomas, and Yoon Nelson's were also evaluated. Increasing a bed height resulted in better removal of Nickel (II) in all 3 models. Therefore, The utilization of Styrofoam-derived activated carbon as a medium for ongoing Nickel (II) adsorption from an aqueous solution.

Keywords: Fixed carbon; Volatile matter; Nickel (II) adsorption; Contact time; Carbon dosage.

1. INTRODUCTION

Styrofoam, a proprietary brand of closed-cell extruded polystyrene foam, boasts a diverse range of applications due to its lightweight composition, consisting primarily of air and possessing buoyancy. It is frequently employed in containers of food, beverages cups, and cushioning material in packaging and as a building insulation board in walls and roofs, serving as both thermal insulation and a barrier against water infiltration. As urban areas expand, the disposal of solid waste has become a critical concern. One significant contributor to this issue is non-biodegradable waste materials like Styrofoam, which have garnered attention due to their detrimental impact on the environment. Styrofoam is a much larger global waste problem. According to EPA and The United States alone generates around 25 billion pounds of Styrofoam waste each year. This is the equivalent of about 2.5 billion foam cups or 20 foam cups per person per year. The global generation rate of Styrofoam waste is difficult to quantify, as it varies significantly from country to country and is not consistently tracked or reported. It is also a type of plastic that is not biodegradable and can take hundreds of years to break down in the environment. When disposed of improperly, it can contribute to pollution and release toxins into the air and water, the International Agency for Research on Cancer states that Styrofoam has a chemical substance that causes cancer in humans. The combustion of Styrofoam can result in the release of toxic compounds like styrene, carbon monoxide, and other deleterious substances.

The Styrofoam is non degradable and easily recyclable. The Styrofoam waste is categorized under plastics hence it occupies majority of place in landfill due to its extruded form. This Styrofoam is more harmful than plastic to the environment. The Styrofoam occupies 30% of space in land fill and its life span to decompose is 500 years [1]. The inadequate disposal of Styrofoam can exacerbate pollution and exacerbate the release of toxins into the environment. The appropriate recycling or disposal of Styrofoam is essential in mitigating its negative impact on both the surroundings and human health. An optimal solution to this problem is the utilization of Styrofoam in the form of activated carbon for environmental applications.

Another significant ecological concern is the presence of heavy metal pollution, which pertains to the accumulation of elevated levels of heavy metals in the environment. Heavy metals are toxic and can have

negative impacts on human health and the ecosystem. Some common heavy metals that can cause pollution include lead, mercury, cadmium, Nickel and chromium. This research aims to remove Nickel (II) from water as it can harm the surroundings and human health. The accumulation of heavy metals like Nickel in the environment poses risks to both ecosystems and human health. These metals can enter water sources through various industrial processes and subsequently contaminate aquatic systems, potentially entering the food chain and posing health hazards. Adsorption is the method used in cleaning the water contaminated with Nickel (II) and meet sustainability goals [2]. The EPA and WHO have set a limit of 0.02 mg/L for Nickel (II) in drinking water. Prolonged exposure to excessive concentrations of water-soluble nickel compounds can potentially result in carcinogenic outcomes, particularly when combined with other carcinogenic chemicals or nickel compounds that are less soluble in aqueous solution. An environmental ramification of metallic ions, like nickel, in aqueous solution in terms of stability, mobility and toxicity, can be substantial. Although there are several techniques employed to extirpate metallic contaminants from effluent, methods such as ion exchange, electrocoagulation, and chemical precipitation may be employed many of them have limitations such as incomplete removal, significant expenses and production of toxic sludge. An alternative and appealing option for heavy metal removal is the adsorption process, which is relatively simple, cost-effective, and efficient.

This study aims to synthesize activated carbon from waste Styrofoam, creating a porous structure with high surface area. This carbon material will be tested for its effectiveness in removing toxic nickel Ni (II) ions from aqueous solutions, contributing to environmental remediation. The research addresses waste management concerns by repurposing Styrofoam, promoting sustainability and reducing pollution. The focus lies on evaluating the carbon's adsorption performance for nickel ions, considering factors like capacity and kinetics. Material characterization techniques will provide insights into its physical, chemical, and structural properties, aiding understanding of its behaviour. Additionally, the study may assess the synthesized carbon's environmental impact and explore its practical applications in water treatment or industrial wastewater management.

2. MATERIALS AND METHODS

2.1. Activate carbon

Activated carbons (ACs) are efficient adsorbents with a broad range of uses. Activated carbon is synthesized by three ways physical activation, chemical activation, and steam activation. Where is physical activation involving only heat to carbonization process and it is quite simple and easy, chemical activation involves the chemical and heat for the carbonization process, and for steam activation involves initial oxidation and followed by steam for its carbonization process. While ACs are highly effective, they are more costly than other adsorbents, limiting their use [3]. This has led to increasing research on producing low-cost activated carbons using economically viable and inexpensive raw materials, that can perform similarly or even better than traditional materials.

2.2. Adsorption process

Adsorption is a process where molecules of a liquid or gas stick to a solid surface through physical or chemical interactions. This involves the use of adsorbents, which are materials that can bind to the heavy metals and remove them from the water. It is also extensively employed in industrial contexts, including but not limited to applications such as activated charcoal, synthetic resins, and water purification [4]. Physical adsorption is the process where weak attractive forces, such as van der Waals forces, bind the adsorbent and adsorbate together. This particular form of adsorption is typically reversible and transpires at relatively low temperatures. Chemical adsorption occurs when strong chemical bonds adsorbent and adsorbate are conjoined via a process known as adsorption. This type of adsorption is typically irreversible and occurs at elevated temperatures. Electrostatic adsorption is when the adsorbate is attracted to the adsorbent due to an electrostatic force, such as Coulombic attraction. It is reversible and can occur at any temperature. The Langmuir-Hinshelwood adsorption mechanism is characterized by the rate of adsorption being limited by the speed at which the adsorbent and adsorbate are chemically react. Freundlich adsorption is distinguished by an inverse proportionality of non-linear correlation exists between the quantity of adsorbate that is adsorbed and an adsorbate concentration present in the solution is the phenomenon of adsorption. It is usually reversible and can occur at any temperature. The Ni (II) adheres primarily to a uniform substrate forming a single layer [5,6].

2.3. Adsorption isotherms

Adsorption isotherms show how much of a substance is adsorbed onto a surface based on pressure or concentration at a certain temperature. Isotherms are important in understanding the equilibrium relationship between the fluid phase concentration and the amount adsorbed at a constant temperature [7]. Isotherms are graphical

representation of the quantity of substance adsorbed versus the pressure or concentration of the substance at a constant temperature or time.

2.4. Kinetic models

The study of adsorption kinetics modelling aims to establish the rate of adsorption and kinetic equations for a specific chemical reaction

Pseudo first order kinetics equation is

$$\ln(q_e - q_t) = \ln q_e - K_1 t \quad (1)$$

where, $K_1(\text{min}^{-1})$ is the equilibrium rate constant and q_t are the adsorption capacity (mg/g) at time t [7].

Pseudo second order kinetics are given by the equation:

$$\frac{t}{q_t} = \frac{1}{k_2 q_e^2} + \frac{1}{q_e} \quad (2)$$

The K_2 ($\text{g mg}^{-1} \text{min}^{-1}$), rate constant for adsorption can be determined by isotherms plots and the suitability of the isotherm and kinetic model can be predicted by R^2 values [7].

2.5. Break through volume

Breakthrough volume in an adsorption column refers to the volume of fluid that has passed through the column before the adsorbent reaches its saturation point and the adsorbate concentration in the effluent exceeds a certain threshold. In other words, it is the point at which the adsorbent can no longer effectively adsorb the adsorbate and it starts to appear in the effluent. It is an integral characteristic in the engineering of adsorption columns, and is utilized to calculate the proportionate dimensions of the column and the quantity of adsorbent required for a particular utilization.

2.6. Column modelling

Adsorption columns are utilized to isolate and purify gases and liquids through adsorption, a process where molecules in a fluid are attracted and retained by a solid or liquid surface. Modelling adsorption columns involves forecasting the behaviour of the fluid as it flows through the column and the molecules adhering to the adsorbent material. This can be achieved by using mathematical models that consider the physico-chemical properties of the fluid, adsorbent material, and conditions under which a column is operated. Adsorption column modelling involves the use of mathematical models to simulate the behaviour of an adsorption column, which is a device used to separate and purify substances using the phenomenon of adsorption. There are various types of adsorption column methods that are utilized in multiple fields of application including Breakthrough curve modelling, Kinetic modelling, Isotherm modelling, Dynamic modelling, Multicomponent modelling, Fixed-bed modelling Moving-bed modelling. This study employs fixed bed mathematical modelling, such as Thomas, Adams-Bohartz, and Yoon-Nelson. Thus, utilization of these models facilitated the extraction of a plethora of parameters that characterize the efficiency of the adsorption column model across a wide range of conditions, including varying bed heights and flow rates.

2.6.1. Thomas modelling

(Thomas, 1944) formulated a adsorption model for which there are no external or internal diffusion constraints. The linearized version of this model, known as the Thomas model, this can be represented in the following manner)

$$\ln\left(\frac{C_0}{C_t} - 1\right) = \frac{k_{Th} q_e W}{Q} - K_{Th} C_0(t) \quad [8]$$

The mathematical expression of the linearized form can be represented as:

where

C_t represents the effluent metal concentration at a given time t (mg/L),

C_0 represents the inlet metal concentration (mg/L),

C_o/C_t represents the ratio of inlet to outlet metal concentrations.

q_e denotes the equilibrium metal uptake (mg/g),

k_{Th} represents the Thomas rate constant (mL/min.mg),

Q represents the inlet flow rate (mL/min)

W represents the mass of adsorbent (g), and

t represents the flow time (min).

A plot of $\ln [(C_o/C_t) - 1]$ vs. time can be used to find q_e and k_{Th} by analyzing the intercept and slope.

2.6.2. Adams-Bohart modelling

The Adams-Bohart model is a mathematical representation developed in the 1950s by J.C. Adams and R.E. Bohart, which describes the attachment of a dissolved substance to a solid surface in an adsorption column. This paradigm is predicated upon the postulates of unidirectional flow and adsorption equilibrium, and can be utilized to approximate the solute's molarity at various junctures along the column throughout the duration of the experiment.

$$\ln \left(\frac{C_t}{C_o} \right) = K_{AB} C_o t - K_{AB} N_o Z / U_o \quad [9]$$

Where

C_t is the outlet metal ion concentration,

C_o is the metal ion concentration,

t is the flow time in (minutes).

K_{AB} is the Kinetic constant or Bohart-Adams rate constant (L/mg min),

Z is the bed depth of the fixed bed column in (cm),

N_o is the Adsorption capacity of the adsorbent (mg/L),

U_o is the superficial velocity in cm/min,

2.6.3. The Yoon -Nelson modelling

This model is an expedient formula that elucidates the adsorption process within columns. With this ideology a minimal amount of specific information pertaining to the corporeal attributes of the column and the characteristics of the adsorbent [10]. This paradigm is devised to elucidate the behaviour of adsorption process in the context of fixed adsorption column and it is simplified as follows,

$$\ln \frac{C_t}{C_o - C_t} = k_{YN}(t) - k_{YN}\tau \quad [8]$$

Wherein,

τ is the time (in minutes) required for 50% adsorbate breakthrough.

k_{YN} is the rate velocity constant (L/min)

A plot of $\ln [C_t/C_o - C_t]$ vs. t was used to find k_{YN} and τ by analyzing the gradient and intercept of the plot.

The Styrofoam waste is procured, reduced to small fragments, dried under solar irradiance to eliminate any extant moisture, and dissolved in toluene. Dissolving Styrofoam in toluene increases the amount of PF carbonized per batch by shrinking the polymer volume by removing air bubbles. The solution obtained is thus dried in hot air oven for 8hrs to remove the moisture present in it. For chemical activation of Styrofoam activated carbon the KOH (potassium hydroxide) is used. The prepared material is pyrolyzed at a different temperature. After the carbonisation process the obtained material is washed several times to remove the char present in it and subjected to various test to find its carbon characteristics. The carbon characterises test was performed as per (IS 877: 1989) [12].

Small fragments of Styrofoam were meticulously excised to amplify the available surface area, thereby facilitating subsequent processing stages. Waste materials were procured and meticulously fragmented before undergoing a drying process employing solar irradiance, thereby effectively eradicating any residual moisture

content. The introduction of toluene as a dissolving agent for the Styrofoam proved instrumental, as it concurrently augmented the carbonization capacity per batch by mitigating the polymer volume through the expulsion of entrapped air bubbles. The ensuing solution was subjected to thorough desiccation within a hot air oven, extending over a duration of 8 hours, to ensure the complete removal of any remaining moisture. In effecting the chemical transformation of Styrofoam into activated carbon, the application of potassium hydroxide (KOH) was embraced. The meticulously prepared material was subsequently subjected to pyrolysis at an array of distinct temperatures. In the aftermath of the carbonization procedure, the resultant substance underwent multiple rounds of meticulous washing, effectively eliminating any vestiges of residual char. Subsequent to this purification phase, an array of assorted tests was meticulously conducted to validate and delineate the carbon characteristics of the material. The execution of the carbon characterization tests adhered rigorously to predefined and meticulous protocols [11].

3. Outcomes and Analyses

3.1. pH

Generally, the pH of all the activated carbon samples is slightly acidic at low temperatures and alkaline at high temperatures. The pH of all the activated carbon ranging from 6 to 8, is suitable for most water treatment applications. Thus, the generated activated carbon samples can be deemed suitable for a plethora of applications that involve adsorption from aqueous solution. This Figure 1, represents the pH of Styrofoam based activated carbon.

3.2. Moisture and ash content

Assaying the moisture content of activated carbon samples ensures that it does not contain an excessive amount of water and is within the desired moisture content range. Ideally, the moisture content of activated carbon should be less than 4% as per (IS 2752:1995) [13]. From the Figure 2, at all activated Styrofoam activated carbon has the moisture content which is less than 5%. The ash content is an intrinsic characteristic of activated carbon that diminishes its efficiency. It denotes the proportion of inorganic particles in the carbon. It was observed an activated carbon samples with an inferior proportion of ash can augment the static carbon content, conversely elevated residue content is detrimental to the activated carbon as it diminishes its stability by impairing its adsorptive capacity. The obtained carbon exhibited an ash content of less than 5 percent as per (IS 2752:1995) [13].

3.3. Fixed carbon and volatile matter

The static carbon content is a solid combustible residue that persists after the application of heat and expulsion of volatilized material. The produced activated carbon has a significant amount of fixed carbon. The volatilized material is an outcome of the organic compounds present in the raw material. Figure 3 indicates the Styrofoam activated carbons have a high percentage of static carbon.

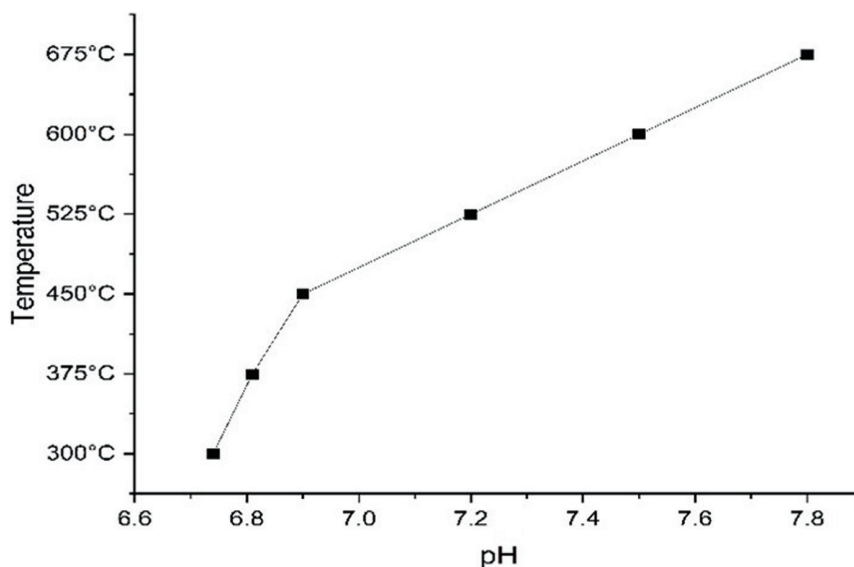


Figure 1: pH of SAC at different temperature.

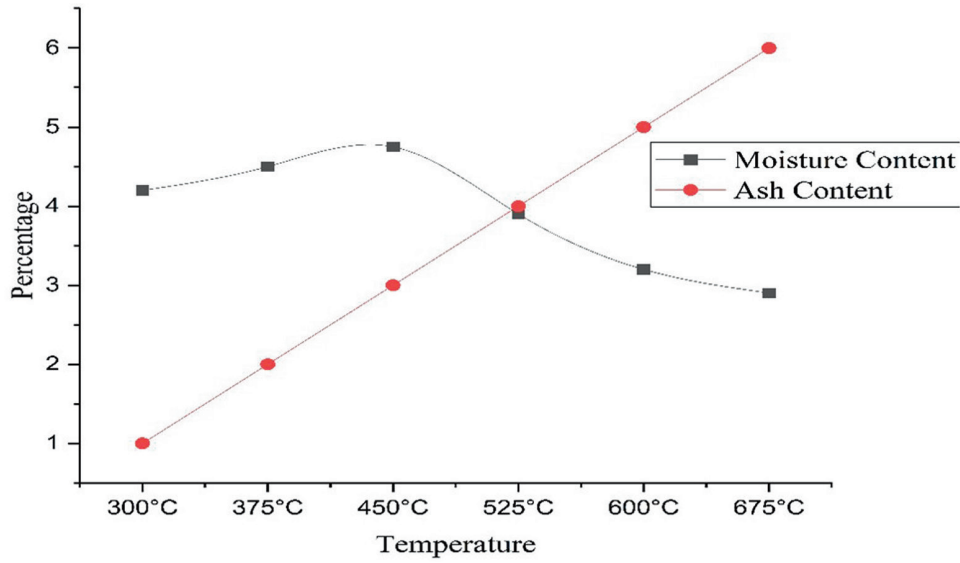


Figure 2: Moisture and Ash Content of SAC at different temperature.

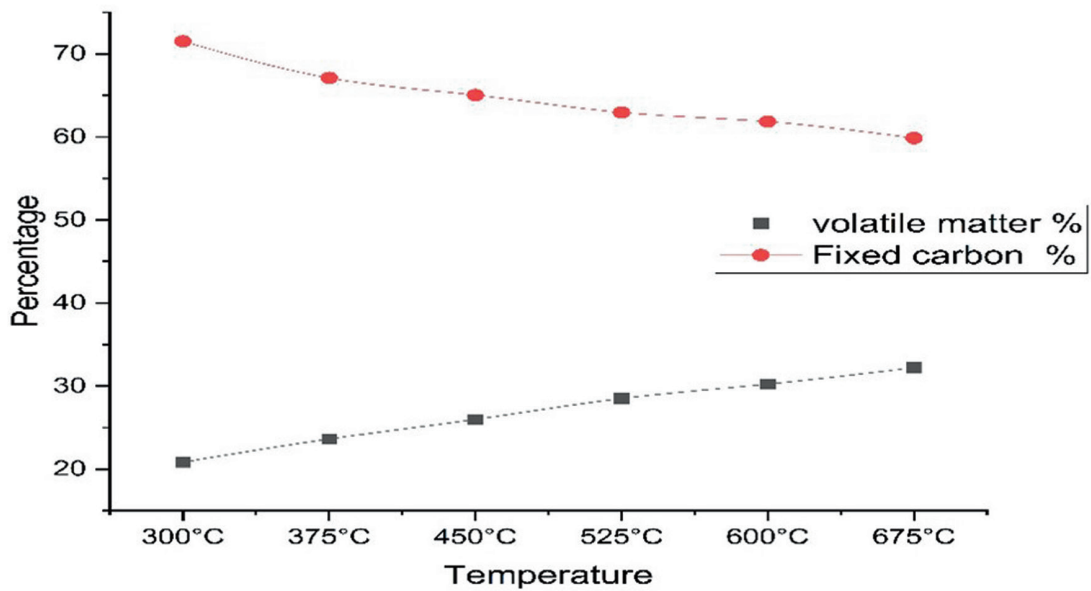


Figure 3: Volatile and Fixed carbon % of SAC at different temperature.

3.4. Methyl blue value

It is an indicator of the adsorption ability of activated carbon. It also aids in determining the expanse of the activated carbon's superficial region. Figure 4 indicates, an attribute of methylene blue above 400 indicates that the carbon is capable of absorbing dye.

3.5. Iodine adsorption

Determining the adsorptive capacity of activated carbon (AC) can be done through a simple and fast technique called iodine adsorption. The measurement of this capacity is known as the iodine number it is typically represented in mg/g, that ranges between 500–1200 mg/g. According to (IS 2752:1995) [13] the iodine adsorption number can provide an approximation of superficial region of AC in m²/g. For AC used in water treatment, it is estimated to have an iodine value in the range of 600–1100 mg/g. The ACs studied in this research have optimal performance for application in purification of water. From the Figure 5 it was found that the obtained activated carbon from Styrofoam has good adsorption property for further study purpose the activate carbon obtained at 525°C is taken and batch experiments are conducted on it.

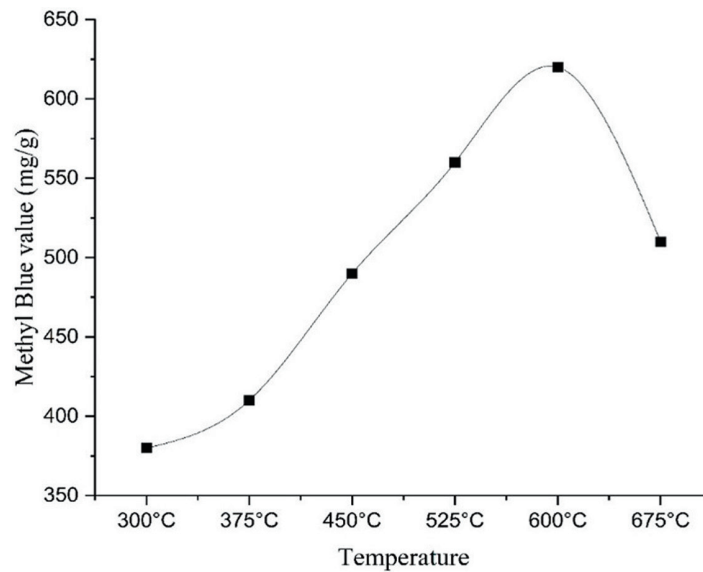


Figure 4: Methyl Blue adsorption value of SAC at different temperature.

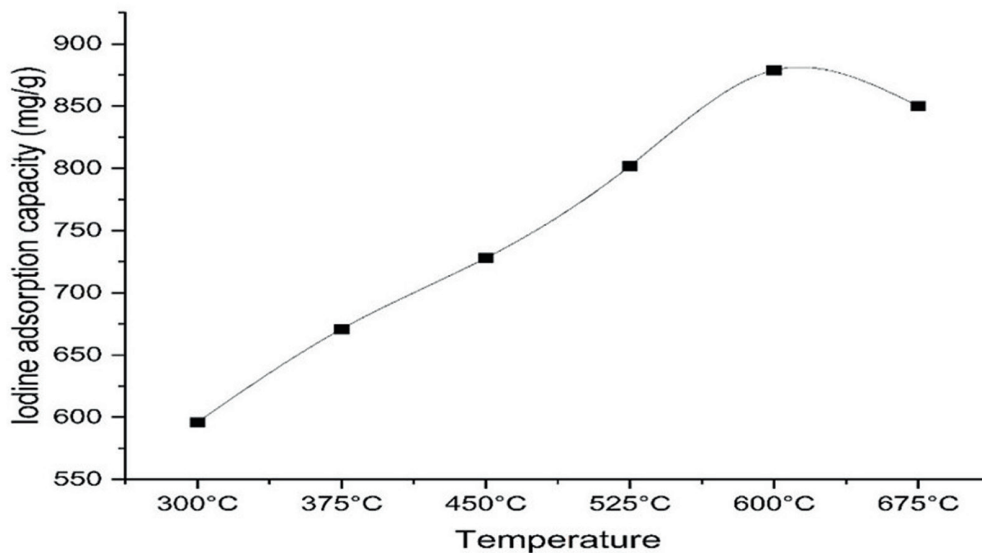


Figure 5: Iodine adsorption value of SAC at different temperature.

3.6. Batch experiments

3.6.1. Effect of pH value

The effluent generated by plating industries often exhibits a broad spectrum of power of hydrogen ion values, making the pH of the system a crucial consideration in the treatment of such waste. The pH of the effluent influences both the chemical composition of the water and the binding sites on adsorbent surfaces. Furthermore, effluent concentration also varies. The experiment was performed with the duration of engagement of 20 minute, a dosage of 0.50g and an agitation speed of 150rpm. Because, as the pH increases more negatively charged surfaces become accessible, thereby promoting greater metal uptake. Figure 6 indicated that the ideal pH for the elimination of Nickel (II) was 7, with a corresponding diminution in adsorption as the pH value augmented.

3.6.2. Impact of Contact time

The utilization of adsorbent dosage as a means to enhance the elimination of heavy metals from water via adsorption processes is a crucial aspect that can impact the treatment's efficacy and proficiency. Increasing the dosage of adsorbent can lead to higher removal efficiency for heavy metals, but it can also result in increased costs and potential adverse effects on the environment. The ideal amount of adsorbent to use is usually identified

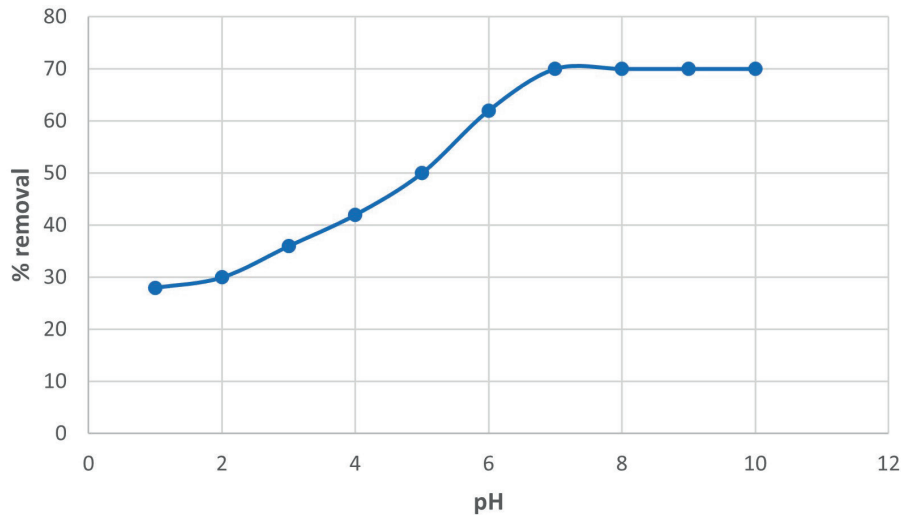


Figure 6: Effect of pH on Nickel (II) removal.

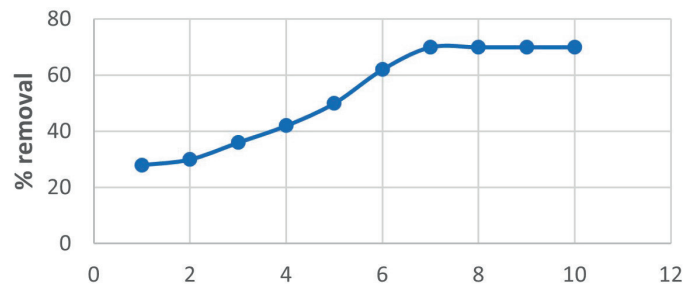


Figure 7: Impact of Contact time on Nickel (II) removal.

through batch testing, and it may vary depending on various elements such as the type of adsorbent, the intrinsic characteristics and quantity of heavy metal, the acidity or basicity of the water (pH), the temperature, and the presence of other dissolved ions in the water [13]. The attaining of equilibrium is a paramount consideration in the engineering of cost-effective wastewater treatment systems. A 50ml solution of nickel with a concentration of 50mg/L was augmented with Styrofoam activated carbon this solution was ascertained through the utilization of Ultra violet Spectrophotometer. The duration of contact was varied from 10 to 120 minutes at an interval of 10 minutes. As the contact time progressed to 60 minutes, there was a steady and gradual decline in concentration. The apex of the removal efficiency was ascertained to be 72% at one hour of interaction duration. From the Figure 7, 60 minutes was taken as optimal duration of contact for Nickel (II) adsorption using Styrofoam as an adsorbate.

3.6.3. Impact of administered adsorbent quantity

An optimization of a quantity of adsorbent is a paramount consideration for facilitating rapid and efficient metal elimination. The quantity of adsorbent employed serves as a crucial determinant in adsorption studies, as it establishes the adsorbent’s capability to adsorb a given initial concentration of nickel ions. The impact of Styrofoam activated carbon on nickel removal is illustrated in Figure 8. The volume of the nickel solution was 50 ml. It was noted that the removal efficiency initially exhibited a gradual decline, owing to the accessibility of active sites, and then demonstrated a slight increase across the range of 0.05–0.50 g. Generally, A higher outcome is observed as the amount of adsorbent increases and quantity of adsorbate being removed from the solution. BARRERA *et al.* [14] illustrates that larger quantity of adsorbent offers a greater surface area for adsorbate to adhere to, consequently there is a higher adsorptive capacity. The optimum dosage was found to be 0.50 g, at the contact time of 30 minutes.

3.6.4. Impact of nickel concentration

The magnitude of nickel present in a solution can have a significant impact on the adsorbent material by modifying the thermodynamic force that propels the process of adsorption. The Nickel concentration in the solution

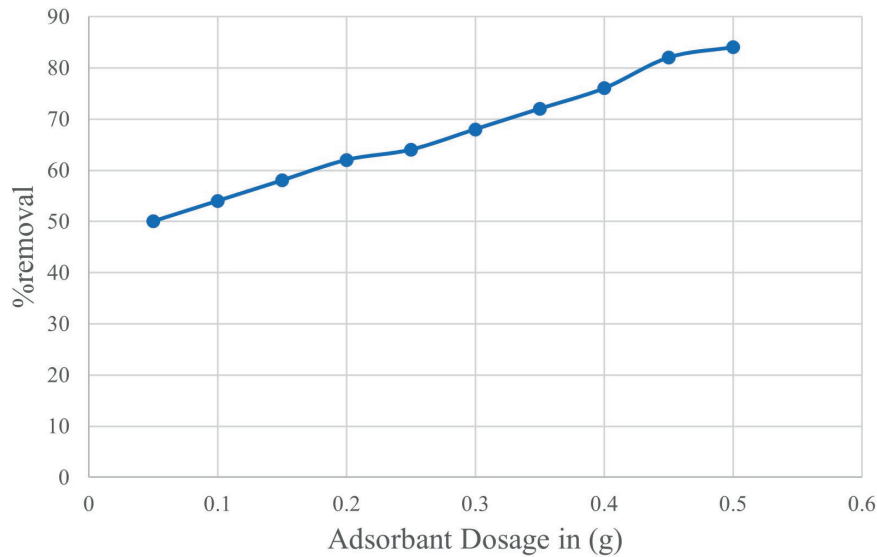


Figure 8: Impact of administered adsorbent quantity.

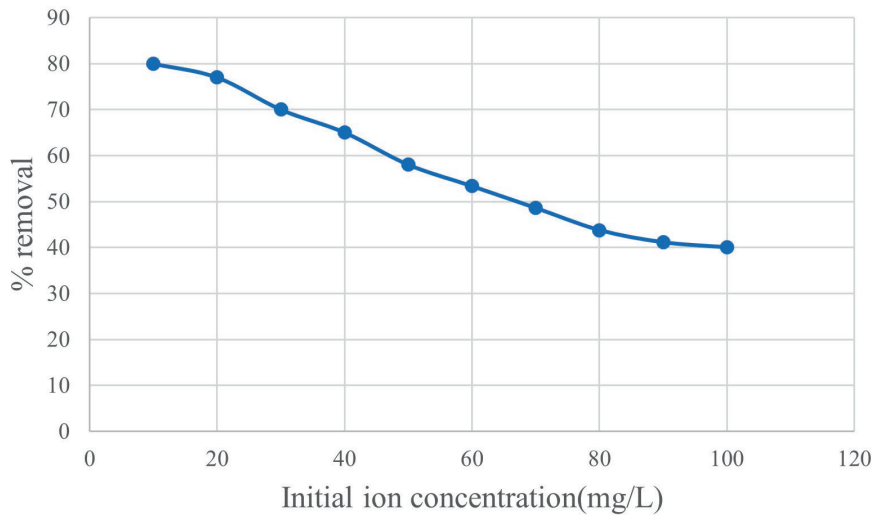


Figure 9: Effect of Concentration of Nickel (II) removal.

can modulate the equilibrium concentration of nickel at the adsorbent’s surface, which subsequently affects the amount of nickel that is adsorbed. Furthermore, the concentration of nickel in the solution can also have an impact on the speed at which adsorption takes place [15]. A higher concentration of nickel in the solution may lead to a faster adsorption rate, while a lower concentration may result in a slower adsorption rate. Thus, the specific effect of concentration of nickel on the adsorbent’s efficacy will be contingent on the traits of the adsorbent substance. It is imperative to take these factors into account when engineering an adsorption system for the elimination of nickel from a solution. An analysis of the initial concentration’s effect was conducted within a spectrum of 10 mg/L to 100 mg/L. The experiment was performed with a most favourable duration of interaction of 60 minutes, with a quantity of 0.50 g, and a pH value of 7. Based on the experimental results, the optimal concentration was determined to be 50 mg/L as shown in Figure 9.

3.6.5. Impact of agitation speed

The manipulation of rotational velocity can enhance the transfer to matter of Nickel (II) ions between the adsorbent surface and main body of the solution. Elevated agitation speeds can facilitate greater mass transfer and an increased rate of adhesion, resulting in increased elimination of Nickel (II) ions from the solution. The swiftness of interaction between the adsorbent and adsorbate plays a crucial role in determining the most effective removal. However, it is important to note that the impact of agitation speed on the elimination of Nickel

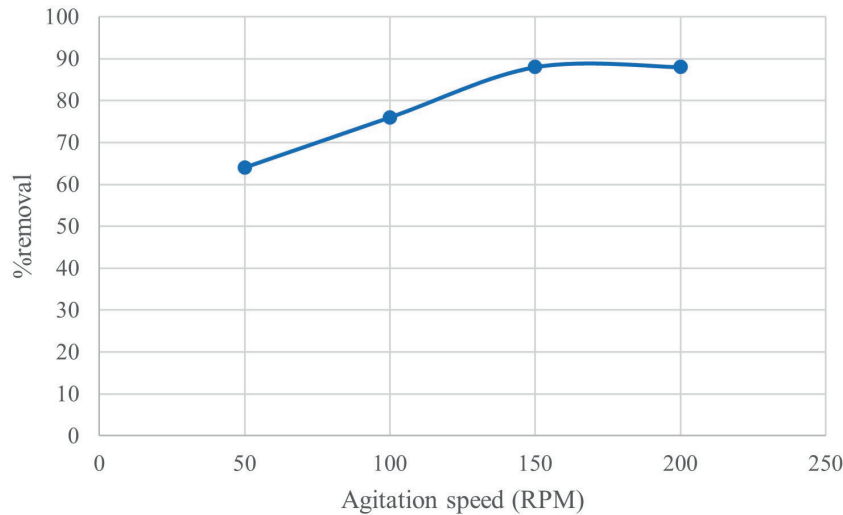


Figure 10: Impact of Agitation speed on Nickel (II) removal.

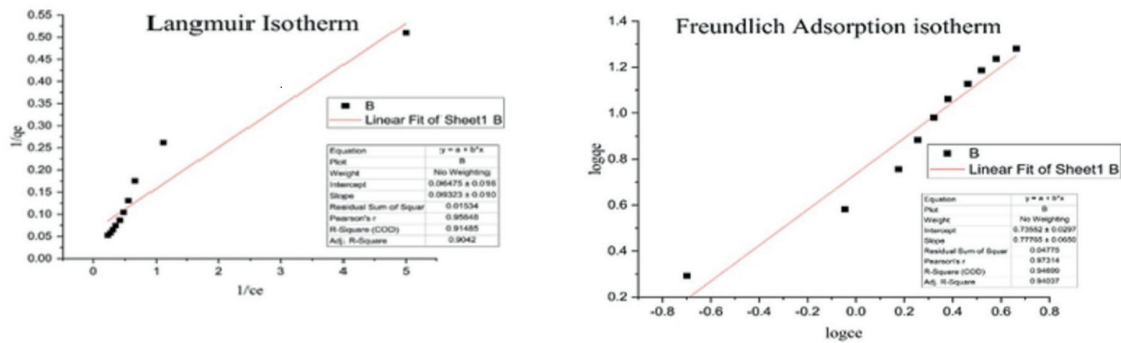


Figure 11: Langmuir and Freundlich Isotherm.

(II) ions may be contingent upon the particular adsorbent material and the conditions of the adsorption process. An impact of agitation speed on the adsorptive of Nickel (II) ions onto an activated carbon has been found to varying. With the higher agitation speeds resulting there was a greater elimination of Nickel (II) ions [16]. The experiment was performed within the range of operating speed of approximately 50–200rpm, with other optimized parameters. As deduced from the Figure 10, the most favourable rotational velocity was determined to be 150 revolutions per minute.

3.7. Adsorption isotherms

The adsorption behaviour of Styrofoam-based activated carbon as an adsorbate was examined using Langmuir and Freundlich’s isotherm models as shown in Figure 11. An isotherm of adsorption provides information about the ability to adsorb, the strength of binding and surface characteristics of the biosorbent, which helps in understanding how the adsorbate binds to biosorbent [17, 18]. q_e was calculated by the equation, $q_e = (C_i - C_e) / (W \times V)$, which is based on the difference between initial and equilibrium adsorbate concentrations, biosorbent weight and solution volume. The percentage of removal efficiency was calculated as $(C_i - C_e) / C_i \times 100$ [18].

The Fredulich isotherm model has demonstrated a notable alignment with experimental data, evident from the substantial coefficient of determination (R^2) at 0.9042. This robust R^2 value indicates a strong linear correlation, suggesting the model’s aptitude in accurately representing the adsorbate’s conduct on the adsorbent surface. However, discerning interpretation of these results requires considering additional influential factors. Upon scrutinizing the comparative analysis of Table 1 and Table 2, it becomes evident that the Langmuir isotherm exhibits lesser congruence with the experimental data compared to the Freundlich isotherm. This disparity is accentuated by the coefficients of linear regression, with the Langmuir isotherm yielding an inferior R^2 value compared to the Freundlich isotherm ($R^2 > 0.9404$ in all cases). This observation lends weight to the proposition that monolayer adsorption of Nickel (II) takes place on Styrofoam-based activated carbon. The Langmuir equation’s parameter, known as the separation factor (RL), assumes values below unity for both isotherms. This underscores the inclination towards adsorption phenomena under the prevalent conditions, as indicated by these

Table 1: Parameters of Langmuir and Freundlich isotherms.

q _{max} (mg/g)	K _L	R _L	R ²	K _L	R _L	R ²
15.4440	0.6945	0.0193	0.9042	1.7490	0.0113	0.9404

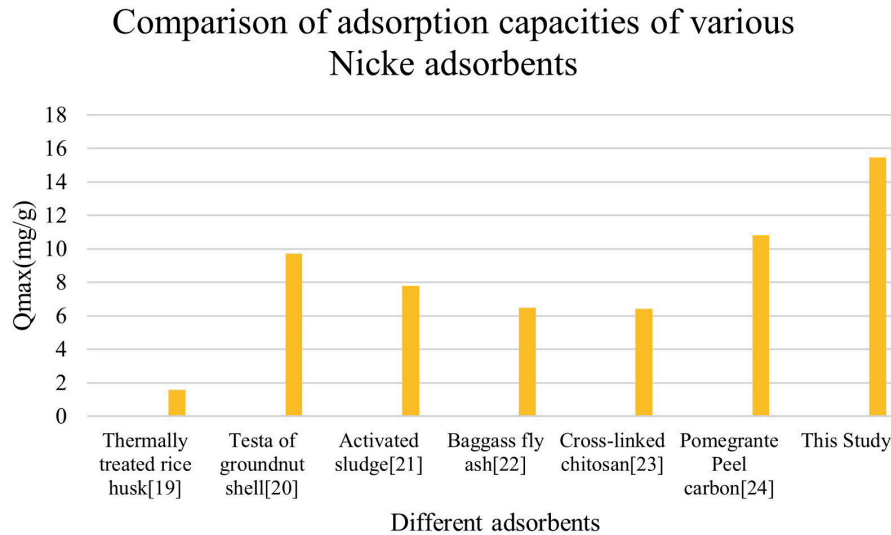


Figure 12: Comparison of Nickel removal using different activated carbons.

RL values. Specifically, an RL range of 0 to 1 signifies a favorable and absorbent milieu [18], further reinforcing the inference of advantageous adsorption tendencies in this context.

The adsorption mechanism between Styrofoam-based activated carbon and nickel (II) involves surface functional groups forming coordination bonds, aided by the material’s porous structure. Chemical affinity, pH, and competitive adsorption influence the process. The calculated adsorption capacity (q_e) of 15.44 mg/g showcases the material’s effectiveness in adsorbing nickel ions. The interaction could be chemisorption or physisorption, driven by factors like surface area and ion charge. Experimentation with varying conditions helps understand optimal adsorption. The interaction between Styrofoam-based activated carbon and the removal of Nickel (II) ions constitutes a multifaceted process involving a delicate balance of physical and chemical forces. The adsorption mechanism is underpinned by an intricate array of factors, including the presence of diverse surface functional groups, ion exchange dynamics, complexation phenomena, chemisorption, and physisorption interactions. These elements collectively orchestrate the efficient sequestration of Nickel (II) from aqueous solutions onto the activated carbon’s surface. The adsorbent’s surface functional groups, replete with oxygen-containing moieties like carbonyl, hydroxyl, and carboxyl groups, play a pivotal role in initiating adsorption. These active sites facilitate ion exchange, enabling the binding of Nickel (II) ions through coordination complexes [19]. This intricate interplay of coordination involves chemisorption, where robust chemical bonds form, and physisorption, driven by relatively weaker van der Waals forces. In this intricate dance of interactions, the Langmuir isotherm’s Q_{max} value, an impressive 15.5 mg/g, quantifies the adsorption capacity with precision as shown in Figure 12. This value underscores the material’s potential as an efficacious adsorbent for Nickel (II) removal. As the adsorption mechanism emerges as a harmonious symphony of chemical affinity and surface reactivity, the intricate choreography of these interactions illuminates the promise of Styrofoam-based activated carbon in addressing waterborne metal ion contamination effectively.

3.8. The pseudo-first-order equation

Lagergren’s rate equation stands as a prominent choice when elucidating the adsorption of substances from a liquid medium. It assumes that the rate at which adsorption occurs is directly linked to the number of available sites on the surface and the number of sites that remain unoccupied. In its linear representation, the pseudo-first-order equation can be presented as follows [26]

$$\log(q_e - qt) = \log q_e - \frac{k_1}{2.303} t \tag{3}$$

The parameter qt (measured in mg/g) represents the quantity of absorbed nickel ions at a given time t , while k_1 (expressed in min^{-1}) stands for the rate constant inherent to the pseudo-first-order model for adsorption. The empirical outcomes regarding the first-order rate constants are outlined in Table 2, which indicated the acquired adsorption data exhibit a suboptimal regression coefficient. This observation implies that the adsorption behaviour of Ni^{2+} onto the activated carbon doesn't conform entirely to the kinetics proposed by the pseudo-first-order model.

3.9. The pseudo-second-order rate equation

The equation for the linearized form of the pseudo-second-order model is as follows [26]

$$\frac{t}{qt} = \frac{1}{K_2 q^2} + t/q \tag{4}$$

Here, k_2 (expressed in units of $\text{g} (\text{mg min})$) signifies the rate constant linked with the pseudo-second-order kinetic model. The correlation between the variables is notably in agreement with the pseudo-second-order equation, as illustrated in Figure 13. The coefficient of correlation r^2 in the linear representation indicates a robust association between the parameters. This observation further underscores that the adsorption process adheres to the kinetics dictated by the pseudo-second-order model, a conclusion reinforced by the data presented in Table 2.

3.10. Adsorption Mechanism

Diffusion models were additionally employed to elucidate the progression of nickel adsorption. The intricate process of solid-liquid sorption involving metal ions and the adsorbent encompasses three primary stages [27] (i) The initial movement of metal ions from the bulk solution to the outer surface of the adsorbent, commonly known as film diffusion; (ii) The subsequent translocation of metal ions within the interstices of the adsorbent, denoted as intraparticle diffusion, materializes as either pore diffusion or solid surface diffusion; (iii) The involvement of active sites on the adsorbent's surface for sequestering metal ions. The intraparticle diffusion model is succinctly expressed through the subsequent equation, encompassing intricate dynamics within its framework [28].

$$qt = K_{\text{diff}} t^{1/2} + C \tag{5}$$

where K_{dif} is the intra-particle diffusion rate constant ($\text{mg}/(\text{g min}^{1/2})$), and C is a constant that gives an idea about the boundary layer thickness (mg/g).

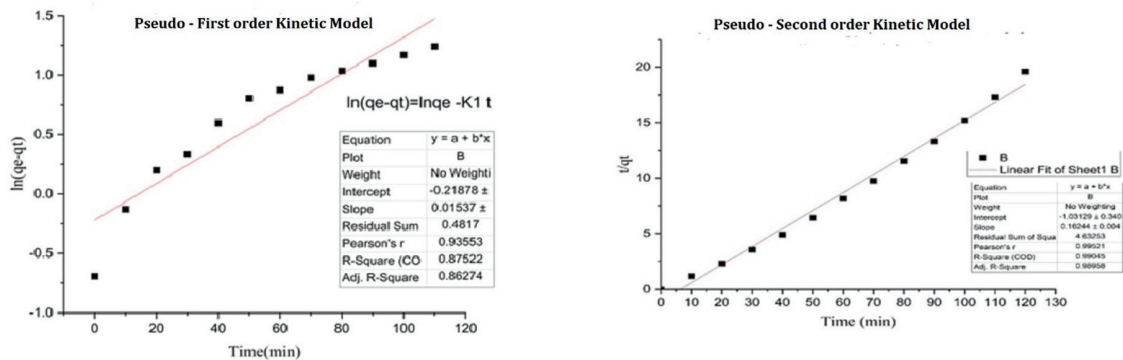


Figure 13: Pseudo- First and Second Order Kinetic Model.

Table 2: Kinetic models.

PSEUDO – FIRST ORDER KINETICS		PSEUDO – SECOND ORDER KINETICS		INTRA PARTICLE DIFFUSION	
$k_1(1/\text{min})$	0.0001	$k^2(\text{g}/\text{mg}/\text{min})$	0.079	$K_{\text{dif}} (\text{mg}/(\text{g min}^{1/2}))$	0.0567
r^2	0.8627	r^2	0.9896	$C (\text{mg}/\text{g})$	6.0837
				r^2	0.96388

The intraparticle diffusion phenomena are visually represented by plotting experimental outcomes, specifically qt against $t^{1/2}$, across distinct adsorbents in Figure 13. The coefficients K_{dif} as well as the correlation coefficients (r^2) extracted from these intraparticle diffusion graphs are presented within Table 2. The C values derived from the intraparticle diffusion framework suggest that this mechanism might not singularly dictate the progression of kinetics in this context. Instead, film diffusion emerges as the principal determinant governing the initial adsorption pace, concurrently providing insights into the boundary layer's thickness.

3.11. Column Modelling

Column modelling was conducted utilizing a fixed-bed configuration [29], employing a glass column measuring 30 cm in length and 1.5 cm in internal diameter. The adsorbent material was meticulously introduced into the column via a known mass of the adsorbent substance. To prevent any inadvertent loss of the adsorbent, a layer of cotton wool was positioned at the column's base. Subsequently, distilled water was passed through the adsorbent bed to eliminate any impurities and entrapped air present within the adsorbent.

Before commencing the experimental procedures, the height of the adsorbent bed was measured. A peristaltic pump was employed to ensure a consistent and predefined flow rate within the column. Throughout the experimental duration, sequential samples of the treated solution were collected at regular intervals. Subsequently, the remaining concentration of the target substance was determined through analysis. From the Equation 3, 4 and 5 the data are being calculated for different height of bed of column and with different flow rate.

3.12. Break through Volume and Time

In fixed bed adsorption with downward flow, feed material undergoes adsorption as it flows through the column. The section of the column where most of the solute is removed is called the zone of adsorption. The length of this zone is subjective and depends on the chosen lower limit of solute concentration. Despite the removal of additional solute as the liquid continuously flows through the column below the adsorption zone, a low concentration of solute still eludes capture and is present in the effluent. As more fluid enters the column, the upper portion of the solid becomes saturated with solute, and the zone of adsorption migrates downward along the column akin to a gradually advancing wave. Eventually, the lower edge of the zone of adsorption reaches the base of the column, resulting in a rapid rise in the solute concentration of the effluent. This point is referred to as the Breakpoint, and the resulting S-shaped curve is known as a breakthrough curve.

The Figure 14, indicates that the configuration and progression of the breakthrough curve were slightly affected by variations in the bed depth. In the initial stages of the fixed-bed column, there was a higher affinity for Nickel (II), however, the concentration of Nickel (II) in the effluent rapidly increased once the breakthrough volume or breakthrough time was reached. As depicted in Figure 14, the breakthrough volume was 294, 303, and 410 with the break through time of 30mins, 40mins and 50mins and the saturation time was found to be 120mins, 130mins, 140mins.

An analysis yielded data indicating that the configuration and progression of the breakthrough curve exhibited slight variations in accordance with an alteration in bed depth. An elevated uptake of Nickel (II)

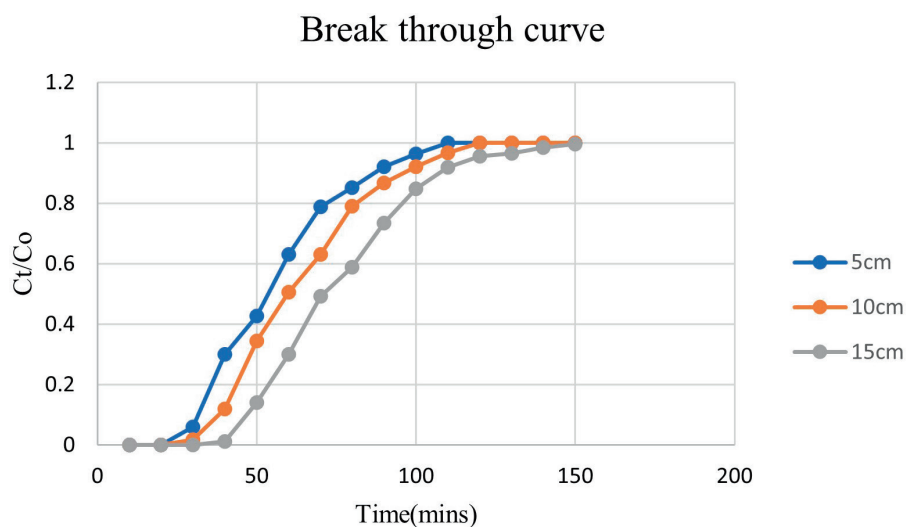


Figure 14: Break through point for the flow rate of 10 ml/min.

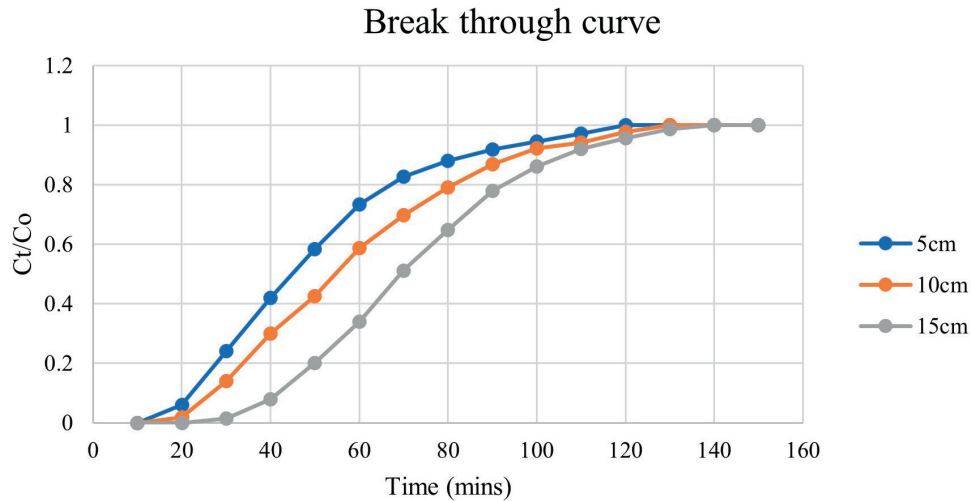


Figure 15: Break through point for flow rate of 15 ml/min.

is discerned at the commencement of the column, yet, concentration of Nickel (II) in the discharge swiftly augmented after the breakthrough volume. The upper bed becomes saturated prior to the lower bed depth. As depicted in Figure 15, the breakthrough volume was 186, 203, and 307 with the break through time of 25mins, 30mins, 40mins and saturation time of 120mins, 130mins, 140mins.

3.13. Adsorption Column Modelling

The data was fitted to the Thomas, Yoon- Nelson and Adams Bhorat column as illustrated in Figure 16 and 17 for the flow rate of 10 mL/min and 15 mL/min flow. The Table (3 and 4) illustrates that as the velocity and height of the bed were augmented, the value of KTH diminished, and conversely, the value of q_o also elevated.

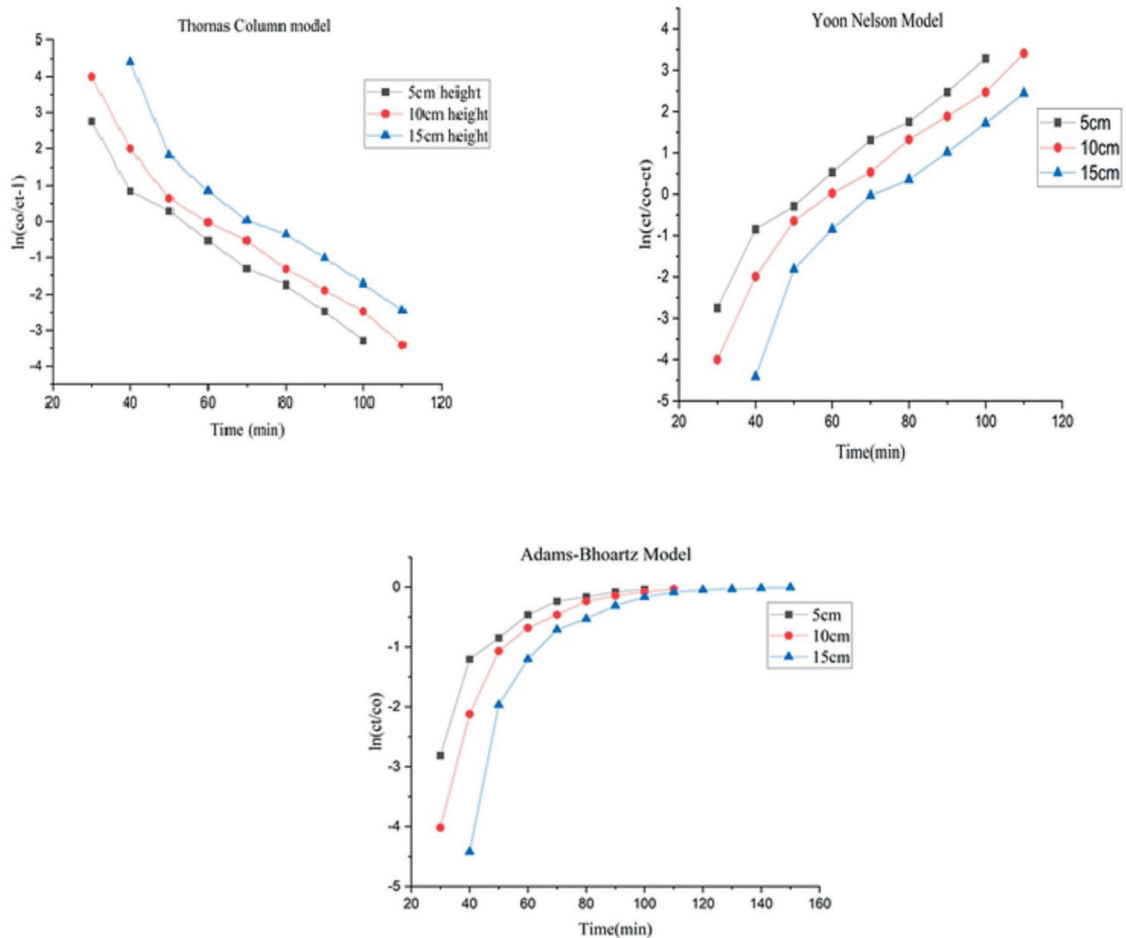


Figure 16: Modelling of the column for a flow rate of 10 mL/min.

In view of this, it can be deduced that the Thomas model posits that the experimental data does not reveal any restricting factors with respect to internal and external diffusion. The K_{AB} and N_o values were determined by analysing the gradient and intercept of the Adams-Bohartz plots in the Table 3 and 4. It was seen that K_{AB} decreased and N_o increased as the depth of the bed increased. The Adams-Bohartz model was observed to be a suboptimal model of fitting, as exemplified by the R^2 values that ranged from 0.558 to 0.709. The K_{YN} and τ were determined by analysing the gradient and intercept of the plot of $\ln(C_t/Co-C_t)$ Vs time. As the bed height increases, K_{YN} increases, and as the flow rate increases, K_{YN} decreases (as shown in the Tables 3 and 4).

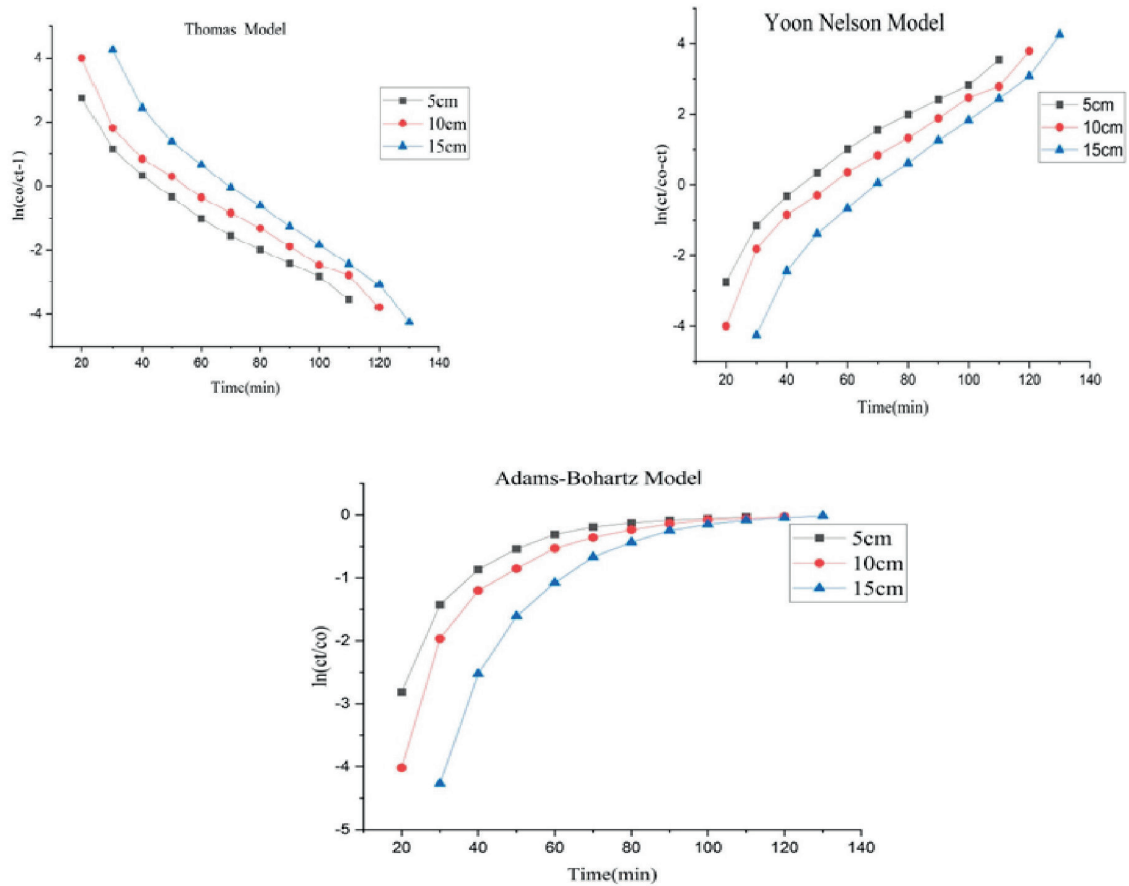


Figure 17: Modelling of the column for a flow rate of 15 mL/min.

Table 3: Impact of flow rate on adsorption model constants.

FLOW RATE 10ml/min	THOMAS CONSTANT			ADAMS-BOHARTZ			YOON-NELSON		
	Bed Height (cm)	K_{TH} (L/mg/min)	q_o (mg/g)	R^2	$K_{AB}(10^{-4})$ (L/mg/min)	N_o (mg/L)	R^2	K_{YN} (min ⁻¹)	τ (mins)
5cm	0.0015	587.41	0.961	6.51	558.07	0.681	0.078	56.27	0.961
10cm	0.0016	678.36	0.945	8.12	1033.32	0.672	0.082	65.94	0.945
15cm	0.0017	775.43	0.905	5.54	888.31	0.558	0.085	77.30	0.905

Table 4: Effect of flow rate on adsorption model.

FLOW RATE 15ml/min	THOMAS CONSTANT			ADAMS-BOHARTZ			YOON-NELSON		
	Bed Height (cm)	K_{TH} (L/mg/min)	q_o (mg/g)	R^2	$K_{AB}(10^{-4})$ (L/mg/min)	N_o (mg/L)	R^2	K_{YN} (min ⁻¹)	τ (mins)
5cm	0.0012	753.5	0.954	5.54	3053.59	0.650	0.068	49.94	0.954
10cm	0.0013	977.86	0.941	5.94	1225.58	0.632	0.066	61.06	0.94
15cm	0.0014	1112.62	0.971	6.92	899.78	0.709	0.0748	74.18	0.971

The increase in τ suggests that the rate at which the adsorbent is depleted is slower, which is beneficial for the adsorption process [30]. The value of τ represents the time required for the adsorbent in the column to reach 50% depletion. A higher value of τ indicates better performance of the column [31–34]. It was also discovered that the observational data exhibited a satisfactory fit with the Yoon-Nelson Model, as evidenced by the R^2 values that ranged from (0.905 to 0.971).

4. CONCLUSION

In the realm of environmental preservation and resource management, the development of innovative and cost-effective materials for water purification and pollutant removal has become paramount. One such remarkable advancement is the synthesis of Styrofoam-based activated carbon, a novel adsorbent material that exhibits exceptional potential for the removal of heavy metals like Nickel (II) from aqueous solutions. This article delves into the synthesis process, characterization, adsorption capabilities, and potential applications of this ground-breaking material. The synthesis of Styrofoam-based activated carbon involved a carefully controlled process conducted at a temperature of 575°C and a pH of 7.2. The material's moisture content, ash content, volatile matter, fixed carbon value, methyl blue value, and iodine value adsorption capacity were meticulously assessed. The moisture content was found to be 3.9%, indicating the material's dryness and stability. The ash content of 4.64% indicated the presence of inorganic residues, while the volatile matter of 28.52% pointed towards the proportion of combustible components. The significant fixed carbon value of 62.94% highlighted the material's carbon-rich composition, which is crucial for effective adsorption. The high methyl blue value of 560 mg/g and iodine value adsorption capacity of 802 mg/g attested to the material's impressive adsorption potential. The ability of the Styrofoam-based activated carbon to remove Nickel (II) ions from aqueous solutions was investigated. The experiments were conducted at pH 7 contact time of 60 minutes, carbon dosage of 0.5 grams, Nickel concentration of 50 milligrams per liter, and an agitation speed of 150 revolutions per minute. The data collected from these experiments indicated the adsorbent's remarkable efficiency in removing Nickel (II) ions, making it a promising material for water purification processes. To further understand the adsorption behaviour, various isotherm models were employed to analyse the experimental data. Among these, the Freundlich isotherm displayed the best fit with an R^2 value of 0.904. From Langmuir isotherm the adsorption capacity of Styrofoam activated carbon was found be 15.5mg/g. The second-order kinetic model demonstrated an excellent suitability for describing the adsorption data, as evidenced by its remarkable coefficient of determination R^2 value of 0.989. A R^2 value of 0.96388 indicates that the intraparticle diffusion model provides a reasonably good fit to the data. Additionally, the Thomas and Yoon-Nelson adsorption models also provided satisfactory fits for the experimental data, emphasizing the consistency and reliability of the material's adsorption capabilities. The synthesis of Styrofoam-based activated carbon presents a significant breakthrough in the field of water treatment and pollutant removal. Its successful synthesis and comprehensive characterization underline its potential as a low-cost adsorbent material. The material's impressive adsorption capabilities for Nickel (II) ions, as demonstrated through various experimental conditions, further solidify its practicality in real-world applications. The utilization of the Freundlich, Kinetic models Thomas, and Yoon-Nelson adsorption models enhances our understanding of its adsorption behaviour and provides a foundation for future studies.

5. BIBLIOGRAPHY

- [1] DAVIS, J.A. *Styrofoam Facts: why you may want to bring your own cup*. Society of Environmental Journalists. <https://www.sej.org/publications/backgrounders/styrofoam-facts-why-you-may-want-bring-your-own-cup>, accessed in July, 2021
- [2] ISLAM, M.A., AWUAL, M.R., ANGOVE, M.J., “A review on nickel (II) adsorption in single and binary component systems and future path”, *Journal of Environmental Chemical Engineering*, v. 7, n. 5, pp. 103305, 2019. doi: <http://dx.doi.org/10.1016/j.jece.2019.103305>.
- [3] KUCUKCONGAR, S., AKBARI, A.J., TURKYILMAZ, M., “Removal of nickel from aqueous solutions using magnetic nanocomposite synthesised with agricultural waste”, *International Journal of Environmental Analytical Chemistry*, v. 102, n. 17, pp. 4996–5014, 2022. doi: <http://dx.doi.org/10.1080/03067319.2020.1790549>.
- [4] CHOUCANE, T., KHIREDDINE, O., BOUKARI, A., “Kinetic studies of Ni (II) ions adsorption from aqueous solutions using the blast furnace slag (BF slag)”, *Journal of Engineering and Applied Sciences (Asian Research Publishing Network)*, v. 68, n. 1, pp. 34, 2021.
- [5] ABD EL-MAGIED, M.O., HASSAN, A.M., GAD, H.M., *et al.*, “Removal of nickel (II) ions from aqueous solutions using modified activated carbon: a kinetic and equilibrium study”, *Journal of Dispersion Science and Technology*, v. 39, n. 6, pp. 862–873, 2018. doi: <http://dx.doi.org/10.1080/01932691.2017.1402337>.

- [6] Wang, Y., & Chao, X., *et al.*, “Removal of nickel (II) ions from aqueous solutions using modified zeolites” *Fresenius Environmental Bulletin*, v.24(12), pp 4316–4321, 2015.
- [7] DIL, E.A., GHAEDI, M., ASFARAM, A., “The performance of nanorods material as adsorbent for removal of azo dyes and heavy metal ions: application of ultrasound wave, optimization and modeling”, *Ultrasonics Sonochemistry*, v. 34, pp. 792–802, 2017. doi: <http://dx.doi.org/10.1016/j.ultsonch.2016.07.015>. PubMed PMID: 27773307.
- [8] LI, G.J., HUANG, X.X., SHI, Y., *et al.*, “Preparation and characteristics of nanocrystalline NiO by organic solvent method”, *Materials Letters*, v. 51, n. 4, pp. 325–330, 2001. doi: [http://dx.doi.org/10.1016/S0167-577X\(01\)00312-3](http://dx.doi.org/10.1016/S0167-577X(01)00312-3).
- [9] RENGARAJ, S., JOO, C.K., KIM, Y., *et al.*, “Kinetics of removal of chromium from water and electronic process wastewater by ion exchange resins: 1200H, 1500H and IRN97H”, *Journal of Hazardous Materials*, v. 102, n. 2–3, pp. 257–275, 2003. doi: [http://dx.doi.org/10.1016/S0304-3894\(03\)00209-7](http://dx.doi.org/10.1016/S0304-3894(03)00209-7). PubMed PMID: 12972242.
- [10] CHEN, S., YUE, Q., GAO, B., *et al.*, “Adsorption of hexavalent chromium from aqueous solution by modified corn stalk: a fixed-bed column study”, *Bioresource Technology*, v. 113, pp. 114–120, 2012. doi: <http://dx.doi.org/10.1016/j.biortech.2011.11.110>. PubMed PMID: 22189077.
- [11] HANBALI, M., HOLAIL, H., HAMMUD, H., “Remediation of lead by pretreated red algae: adsorption isotherm, kinetic, column modelling and simulation studies”, *Green Chemistry Letters and Reviews*, v. 7, n. 4, pp. 342–358, 2014. doi: <http://dx.doi.org/10.1080/17518253.2014.955062>.
- [12] INDIAN STANDARD. *IS 877: Indian Standard Activated Carbons, Powdered and Granular: Methods of Sampling and Test*, New Delhi, IS, 1989
- [13] INDIAN STANDARD. *IS 2752: Indian Standard Activated Carbons, Granular—Specification*, New Delhi, IS, 1995.
- [14] BARRERA, H., UREÑA-NÚÑEZ, F., BILYEU, B., *et al.*, “Removal of chromium and toxic ions present in mine drainage by Ectodermis of Opuntia”, *Journal of Hazardous Materials*, v. 136, n. 3, pp. 846–853, 2006. doi: <http://dx.doi.org/10.1016/j.jhazmat.2006.01.021>. PubMed PMID: 16504390.
- [15] ALSEWAILEH, A.S., USMAN, A.R., AL-WABEL, M.I., “Effects of pyrolysis temperature on nitrate-nitrogen (NO₃–N) and bromate (BrO₃–) adsorption onto date palm biochar”, *Journal of Environmental Management*, v. 237, pp. 289–296, 2019. doi: <http://dx.doi.org/10.1016/j.jenvman.2019.02.045>. PubMed PMID: 30802753.
- [16] LI, S., ZHANG, X., HUANG, Y., “Zeolitic imidazolate framework-8 derived nano porous carbon as an effective and recyclable adsorbent for removal of ciprofloxacin antibiotics from water”, *Journal of Hazardous Materials*, v. 321, pp. 711–719, 2017. doi: <http://dx.doi.org/10.1016/j.jhazmat.2016.09.065>. PubMed PMID: 27701060.
- [17] HUANG, R., MA, X., LI, X., *et al.*, “A novel ion-imprinted polymer based on graphene oxide-mesoporous silica nanosheet for fast and efficient removal of chromium (VI) from aqueous solution”, *Journal of Colloid and Interface Science*, v. 514, pp. 544–553, 2018. doi: <http://dx.doi.org/10.1016/j.jcis.2017.12.065>. PubMed PMID: 29291553.
- [18] HERNÁNDEZ-BARRETO, D.F., RODRIGUEZ-ESTUPIÑÁN, J.P., MORENO-PIRAJÁN, J.C., *et al.*, “Adsorption and photocatalytic study of phenol using composites of activated carbon prepared from onion leaves (*Allium fistulosum*) and metallic oxides (ZnO and TiO₂)”, *Catalysts*, v. 10, n. 5, pp. 574, 2020. doi: <http://dx.doi.org/10.3390/catal10050574>.
- [19] AYUB, A., RAZA, Z.A., MAJEED, M.I., *et al.*, “Development of sustainable magnetic chitosan biosorbent beads for kinetic remediation of arsenic contaminated water”, *International Journal of Biological Macromolecules*, v. 163, pp. 603–617, 2020. doi: <http://dx.doi.org/10.1016/j.ijbiomac.2020.06.287>. PubMed PMID: 32629050.
- [20] FARHAN, A.A., ONG, K.K., YUNUS, W.W., *et al.*, “Optimisation of nickel (II) adsorption using thermally treated rice husk”, *International Journal of Applied Environmental Sciences*, v. 11, n. 3, pp. 717–730, 2016.
- [21] AJMAL, M., RAO, R.A.K., AHMAD, J., *et al.*, “The use of testa of groundnut shell (*Arachis hypogea*) for the adsorption of Ni (II) from the aqueous system”, *Journal of Environmental Science & Engineering*, v. 48, n. 3, pp. 221–224, 2006. PubMed PMID: 17915788.
- [22] HAMMAINI, A., GONZÁLEZ, F., BALLESTER, A., *et al.*, “Biosorption of heavy metals by activated sludge and their desorption characteristics”, *Journal of Environmental Management*, v. 84, n. 4, pp. 419–426, 2007. doi: <http://dx.doi.org/10.1016/j.jenvman.2006.06.015>. PubMed PMID: 16979281.

- [23] SRIVASTAVA, V.C., MALL, I.D., MISHRA, I.M., “Equilibrium modelling of single and binary adsorption of cadmium and nickel onto bagasse fly ash”, *Chemical Engineering Journal*, v. 117, n. 1, pp. 79–91, 2006. doi: <http://dx.doi.org/10.1016/j.cej.2005.11.021>.
- [24] TAN, S., WANG, Y., PENG, C., *et al.*, “Synthesis and adsorption properties for metal ions of crosslinked chitosan acetate crown ethers”, *Journal of Applied Polymer Science*, v. 71, n. 12, pp. 2069–2074, 1999. doi: [http://dx.doi.org/10.1002/\(SICI\)1097-4628\(19990321\)71:12<2069::AID-APP17>3.0.CO;2-S](http://dx.doi.org/10.1002/(SICI)1097-4628(19990321)71:12<2069::AID-APP17>3.0.CO;2-S).
- [25] KHAWAJA, M., MUBARAK, S., ZIA-UR-REHMAN, M., *et al.*, “Adsorption studies of pomegranate peel activated charcoal for nickel (II) ion”, *Journal of the Chilean Chemical Society*, v. 60, n. 4, pp. 2642–2645, 2015. doi: <http://dx.doi.org/10.4067/S0717-97072015000400003>.
- [26] LAGERGREN, S., “Zur theorie der sogenannten adsorption gelöster stoffe. Kungliga svenska vetenskapsakademiens”, *Handlanger*, v. 24, pp. 1–39, 1898.
- [27] HO, Y.S., MCKAY, G., “Kinetic models for the sorption of dye from aqueous solution by wood”, *Process Safety and Environmental Protection*, v. 76, n. 2, pp. 183–191, 1998. doi: <http://dx.doi.org/10.1205/095758298529326>.
- [28] KALAVATHY, M.H., KARTHIKEYAN, T., RAJGOPAL, S., *et al.*, “Kinetic and isotherm studies of Cu (II) adsorption onto H₃PO₄-activated rubber wood sawdust”, *Journal of Colloid and Interface Science*, v. 292, n. 2, pp. 354–362, 2005. doi: <http://dx.doi.org/10.1016/j.jcis.2005.05.087>. PubMed PMID: 16040040.
- [29] WEBER JUNIOR, W.J., MORRIS, J.C., “Kinetics of adsorption on carbon from solution”, *Journal of the Sanitary Engineering Division*, v. 89, n. 2, pp. 31–59, 1963. doi: <http://dx.doi.org/10.1061/JSEDAI.0000430>.
- [30] SINGH, S.K., KATORIA, D., MEHTA, D., *et al.*, “Fixed bed column study and adsorption modelling on the adsorption of malachite green dye from wastewater using acid activated sawdust”, *International Journal of Advanced Research*, v. 3, n. 7, pp. 521–529, 2015.
- [31] KARA, A., DEMIRBEL, E., “Kinetic, isotherm and thermodynamic analysis on adsorption of Cr (VI) ions from aqueous solutions by synthesis and characterization of magnetic-poly (divinylbenzene-vinylimidazole) microbeads”, *Water, Air, and Soil Pollution*, v. 223, n. 5, pp. 2387–2403, 2012. doi: <http://dx.doi.org/10.1007/s11270-011-1032-1> PubMed PMID: 22707803.
- [32] OMITOLA, O.B., ABONYI, M.N., AKPOMIE, K.G., *et al.*, “Adams-Bohart, Yoon-Nelson, and Thomas modeling of the fix-bed continuous column adsorption of amoxicillin onto silver nanoparticle-maize leaf composite”, *Applied Water Science*, v. 12, n. 5, pp. 1–9, 2022. doi: <http://dx.doi.org/10.1007/s13201-022-01624-4>.
- [33] YAGUB, M.T., SEN, T.K., AFROZE, S., *et al.*, “Fixed-bed dynamic column adsorption study of methylene blue (MB) onto pine cone”, *Desalination and Water Treatment*, v. 55, n. 4, pp. 1026–1039, 2015. doi: <http://dx.doi.org/10.1080/19443994.2014.924034>.
- [34] HEIDARINEJAD, Z., DEHGHANI, M.H., HEIDARI, M., *et al.*, “Methods for preparation and activation of activated carbon: a review”, *Environmental Chemistry Letters*, v. 18, n. 2, pp. 393–415, 2020. doi: <http://dx.doi.org/10.1007/s10311-019-00955-0>.